

Pesquisas em Geociências

<http://seer.ufrgs.br/PesquisasemGeociencias>

Chemical Analyses of Zircons in Sequential Sections: An Integrated Electron Microprobe, Backscattered Electron and Cathodoluminescence Image Investigation

Léo Hartmann, Marcos Vasconcellos, Anabela Porto Rosa
Pesquisas em Geociências, 26 (1): 59-66, maio/ago., 1999.

Versão online disponível em:

<http://seer.ufrgs.br/PesquisasemGeociencias/article/view/21134>

Publicado por

Instituto de Geociências



Portal de Periódicos
UFRGS

UNIVERSIDADE FEDERAL
DO RIO GRANDE DO SUL

Informações Adicionais

Email: pesquisas@ufrgs.br

Políticas: <http://seer.ufrgs.br/PesquisasemGeociencias/about/editorialPolicies#openAccessPolicy>

Submissão: <http://seer.ufrgs.br/PesquisasemGeociencias/about/submissions#onlineSubmissions>

Diretrizes: <http://seer.ufrgs.br/PesquisasemGeociencias/about/submissions#authorGuidelines>

Data de publicação - maio/ago., 1999.

Instituto de Geociências, Universidade Federal do Rio Grande do Sul, Porto Alegre, RS, Brasil

Chemical Analyses of Zircons in Sequential Sections: An Integrated Electron Microprobe, Backscattered Electron and Cathodoluminescence Image Investigation

LÉO A. HARTMANN¹; MARCOS A. Z. VASCONCELLOS² & ANABELA PORTO ROSA¹

¹ Instituto de Geociências, Universidade Federal do Rio Grande do Sul, Caixa Postal 15001
CEP 91500-000 Porto Alegre, RS, Brazil. afraneo@if.ufrgs.br

² Instituto de Física, Universidade Federal do Rio Grande do Sul, Caixa Postal 15051
CEP 91500-000 Porto Alegre, RS, Brazil. marcos@if.ufrgs.br

(Recebido em 03/99. Aceito para publicação em 06/99)

Abstract – The three dimensional internal structure and distribution of trace elements of zircon are clarified from the observation of backscattered electron and cathodoluminescence images of zircon plus electron microprobe quantitative determinations of U, Y and Hf. Successive (100) and (001) sections of zircon crystals were investigated in two slightly sheared posttectonic Cambrian granites from southernmost Brazil. Fractures are sealed, and the chemical modifications are seen to migrate into euhedral bands and even larger volumes of the crystals – the contents of U and Hf usually increase significantly, and Y variably so. The sealing of fractures present in one section is observed to evolve to euhedral banding in the next, tying the two features to the same genetic process.

Key words - Zircon, sequential sectioning, backscattered electrons, cathodoluminescence, electron microprobe, chemical analyses.

INTRODUCTION

The observation of the internal structure of zircon in three dimensions is essential for the correct interpretation of the sequence of events affecting the crystal and the containing rock unit, with important consequences for the description of the mineralogical, petrological and geochronological evolution. This can be done by studies of successive sections of zircon obtained by repeated polishing of the mount.

We thus make the chemical and structural description of successive sections of zircon by backscattered electron and cathodoluminescence images of crystals and electron microprobe analyses. This is a useful and novel technique for the description of the three-dimensional structure and chemistry of zircon. Although this important mineral has been extensively studied, some major problems remain unsolved. For instance, is U (and Hf, Y, Th, Pb) only lost from the mineral during hydrothermal alteration, or might it also be added during such an event?

The distribution (and redistribution) of some of these elements in zircon has been studied by Hartmann *et al.* (1997), who demonstrated that Hf, U, Y may be added to the structure of zircon from circulating fluids. They concluded that infiltration is very

active along fractures in many crystals. This process is studied in this article and expanded to the diffusion along euhedral bands. The three-dimensional observation of zircon composition and structure revealed by this technique, used for the first time in this study, concentrates on the relationship between discordant and concordant replacement of old by new zircon, particularly the exchange of Hf, Y and U between the crystal and the fluid. This investigation adds a third dimension to the previous planar studies, which were restricted to (100) sections. The (001) direction of the zircon crystals is now investigated in successive sections.

METHODOLOGY

In order to restrain the geological variables to only two – magmatism and metamorphism, two posttectonic granitic bodies were selected for the investigation, both ca. 550 Ma old (Remus *et al.*, 1997). We did this to simplify the experiment, because in nature more than just two processes have commonly occurred. The intrusive bodies are the Tuna Granite and the São Sepé Granite in the State of Rio Grande do Sul, Brazil. They are both posttectonic to the Brasiliano Cycle and were not affected by the strong 750-700 Ma-old deformation observed in other granitic bodies in the region

Em respeito ao meio ambiente, este número foi impresso em papel branqueado por processo parcialmente isento de cloro (ECF)

and dated by Babinski *et al.* (1996) and Leite *et al.* (1998). The Tuna Granite (Gastal *et al.*, 1992) is part of the Santo Afonso Suite, intrusive into high-grade rocks, whereas the São Sepé Granite is intrusive into low-grade schists; both caused thermal effects on the country rocks. They have only been affected by diffuse low-grade shear-zone metamorphism since emplacement.

Approximately 5 kg of two samples of rock, one from each granite body, were crushed, milled and sieved. Over 300 grains of zircon from each sample were concentrated by mechanical, hydraulic and electromagnetic procedures at the Mineral Separation Laboratory, Universidade do Estado de São Paulo / Rio Claro. Forty crystals were chosen from the samples because they seemed to be most typical of the two granites. These forty crystals were mounted on thin sections, about half with the *c* axis lying horizontally and half vertically. Of the forty, five were studied in detail because they have the most complex petrologic history. The preparation of mounts with horizontal *c* axis is straightforward, for zircons in these samples have 3:1 length to width ratios, as is typical for igneous crystals, and tend to fall (100)-face down on the mount. On the other hand, the preparation of sections perpendicular to the *c* axis required more elaborate procedures (Tab. 1). With this procedure, sections perpendicular to the *c* axis may be studied. After carbon coating, images were made by the backscattered electron (BSE) mode and also of cathodoluminescence (CL), which is an accessory on the Cameca SX-50 EPMA available at "Centro de Estudos em Petrologia e Geoquímica, Instituto de Geociências, Universidade Federal do Rio Grande do Sul" in Porto Alegre. In sequence, the mounts were repolished and new BSE/CL images made. Between two and four polishings of the same crystal were made.

The contents of Hf, Y and U were determined by WDS profiles in selected tomographic planes; analytical conditions used for the stepwise scan across each crystal were 25 kV for electron beam acceleration voltage and 100 nA for current. A 1 µm beam diameter was moved in steps of 0.5 µm along the sample in order to smooth the signal. In some selected points, the characteristic emission lines for Hf, Y and U were acquired using 25 kV, 100 nA and 50 sec per λ with steps of 0.0002 (in $\sin \theta$). Intensities for each element from the spot scan in the samples were compared with the same emission lines obtained from known standards, using the same experimental conditions. No matrix correction was used to determine the concentration in wt%. Precision and accuracy of the results are

approximately $\pm 10\%$ (1σ). Standards used were synthetic UO_2 and a synthetic glass for U and synthetic glass for Hf and Y. In this manner, chemical analyses were made on (100) and (001) sections of crystals.

SEQUENTIAL SECTIONS

The most significant aspect observed is the transition of discordant fracture sealing to concordant euhedral banding. In previous studies, Hartmann *et al.* (1997) communicated the discovery that the content of Hf, Y and U of zircon increases along fractures sealed by percolating fluids.

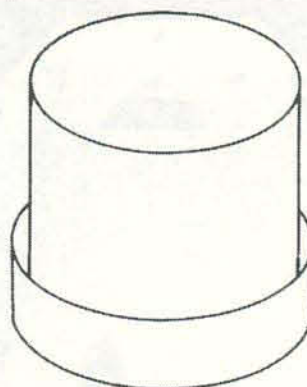
BSE images illustrate more clearly the relationships of the fractures to the crystals and are preferred in this study over CL images, for the latter tend to conceal them. Both types of images are nevertheless useful and are shown for some grains. Figures 1 and 2 (both Tuna Granite) and figure 3 (São Sepé Granite) illustrate key features. The sealing of fractures is present in many places in all four grains; the newer material is lighter gray in BSE images. In crystal 1, several fractures are interrupted by new material along the rims, leaving a remnant fracture in the mantle or core. New material takes up a large volume of core in crystal 1 (lower left in Fig. 1A), a large volume around the inclusion in crystal 2 (lower right of Fig. 1E), and a large core of crystals 3 (Figs. 2A and 2C) and 4 (Figs. 3A, 3B). In figures 2C, 2D, a small mineral inclusion caused deformation of the zircon crystal lattice around the inclusion; the new material of bright/BSE aspect similar to the large core occupied the defect-rich volume around the inclusion.

Euhedral banding is encountered in the upper and right parts of Crystal 1 (Figs. 1A and 1B), left and upper part (mantle) of crystal 2 (Fig. 1E), the left mantle of crystal 3 (Figs. 2A, 2C) and the right rim of crystal 4 (Figs. 3B and 3C). The transition from discordant to concordant substitution is seen on the left and upper part of crystal 2 (Figs. 1C and 1E). In crystal 3, the large new core of figure 2A expands to a euhedral mantle on the left, leaving a dark/BSE fractured remnant of the older magmatic zircon in between. This remnant portion vanishes in the following section (Fig. 2C), in which the core is seen to have diffused to a larger volume and have become more euhedral.

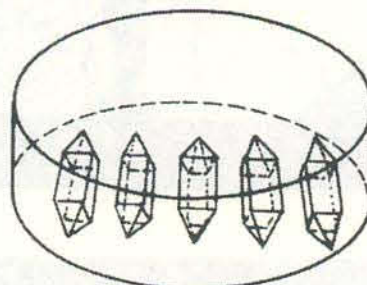
The two sections of crystal 4 are enlightening regarding the transition of discordant to euhedral substitution of old by new zircon. In Fig. 3A, the bright/BSE young nucleus is nearly euhedral, whereas in Fig. 3B it is discordant. Its prism faces are still parallel, but the termination of the core is no longer parallel to

Table 1. Sample separation of zircon with c axis in vertical position

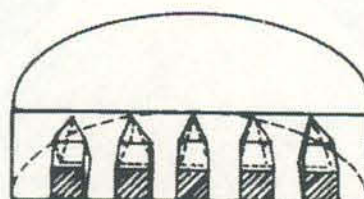
a. Resin is prepared using Struers Epofix Kit, Resin and Hardner. Hardner to resin in 2:15 proportion, warmed for 1 minute at 45°C. Zircon crystal are captured with a needle containing a small drop of this resin and deposited parallel to c axis in a 2.54 cm diameter sample holder and covered with a thin Epofix film. Lateral view.



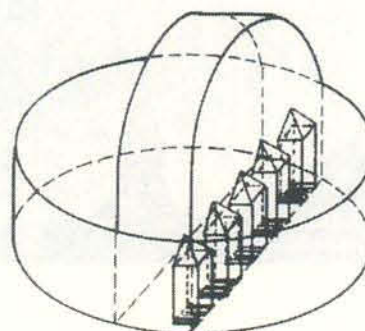
b. After two hours in an oven at 45°C, the zircon crystals are covered with Epofix to 0.5 cm height. The sample holder is then taken to an oven at 45°C for approximately 8 h.



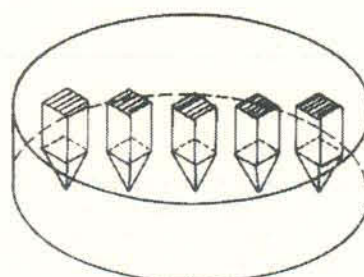
c. Under the binocular, a line is traced across the top of the crystals for sectioning of the resin. The rough sectioned surface is polished with a Struers paper #800. Position of the crystals after sectioning.



d. The half-section containing the crystals is placed face-down in the sample holder and covered with resin to 0.5 cm height. This is taken to an oven at 45°C for 8 h.



e. Excess resin on the top surface of sample is cut off. The lower surface contains the zircon crystals and is polished in the following sequence of Struers paper #320, 500, 800, 2400 and 4000. Next, Struers diamond paste #15, 6, 1 and ¼ μm.



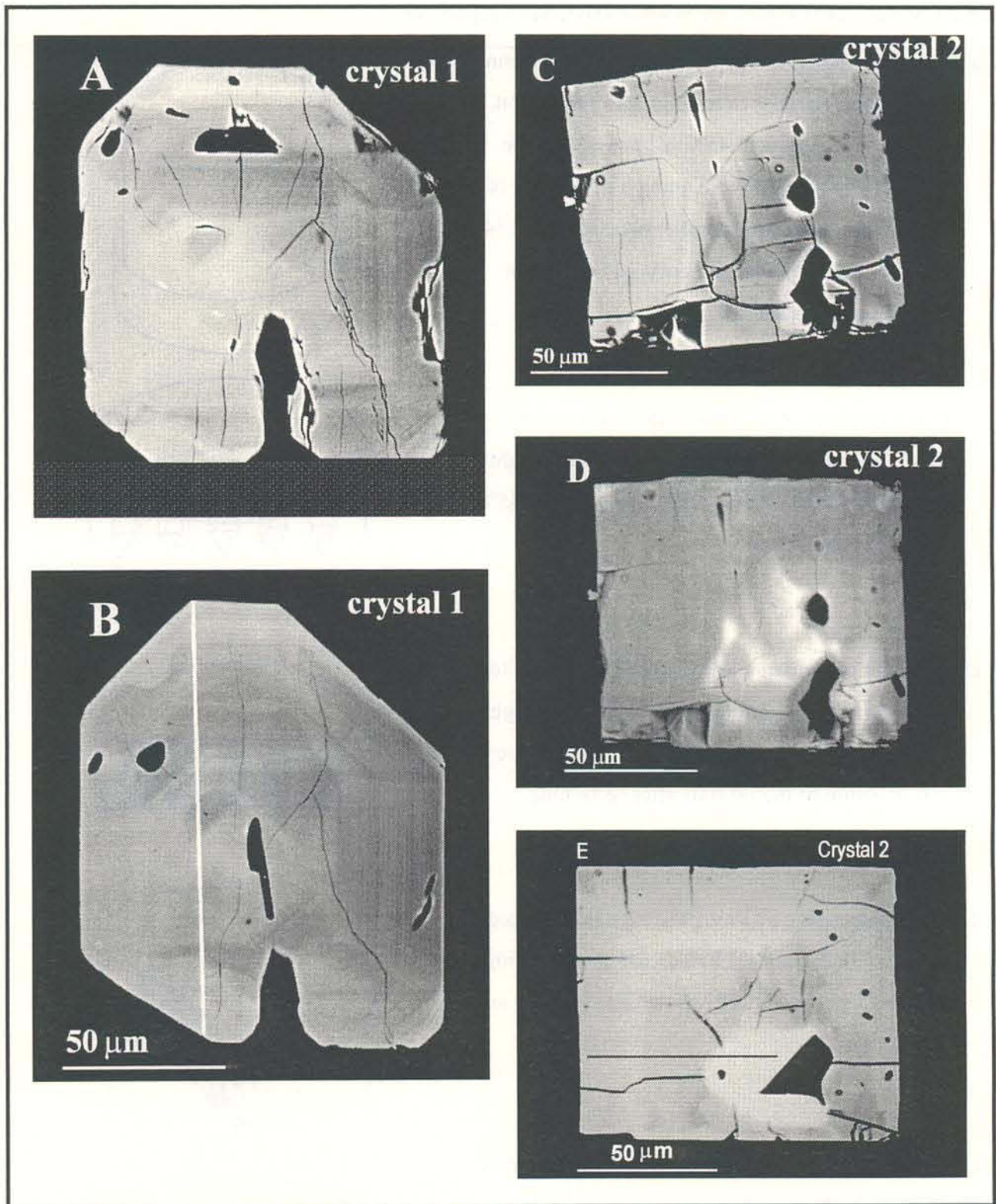


Figure 1 - Tuna Granite zircons in sequential sections. 1A - BSE image of prismatic section of crystal 1, showing large bright (in BSE) region in lower left and center which seals fractures and is euhedral in the core. 1B - BSE image of same crystal 1, displaying modifications in the distribution of the bright area; scan line indicated. 1C - BSE image of crystal 2 in section perpendicular to *c* axis, in which a large and diffuse bright (in BSE) area on the left and upper part does not follow crystallographic directions. 1D - CL image of the same section as 1C; CL-emitting elements (Dy?) re-distributed within the crystal by the fluid-aided diffusion process. 1E - BSE image of crystal 2; the bright (in BSE) portions on the left and upper part have become euhedral in this plane; a large volume has been taken by new zircon around the inclusion on the lower right; scan line indicated.

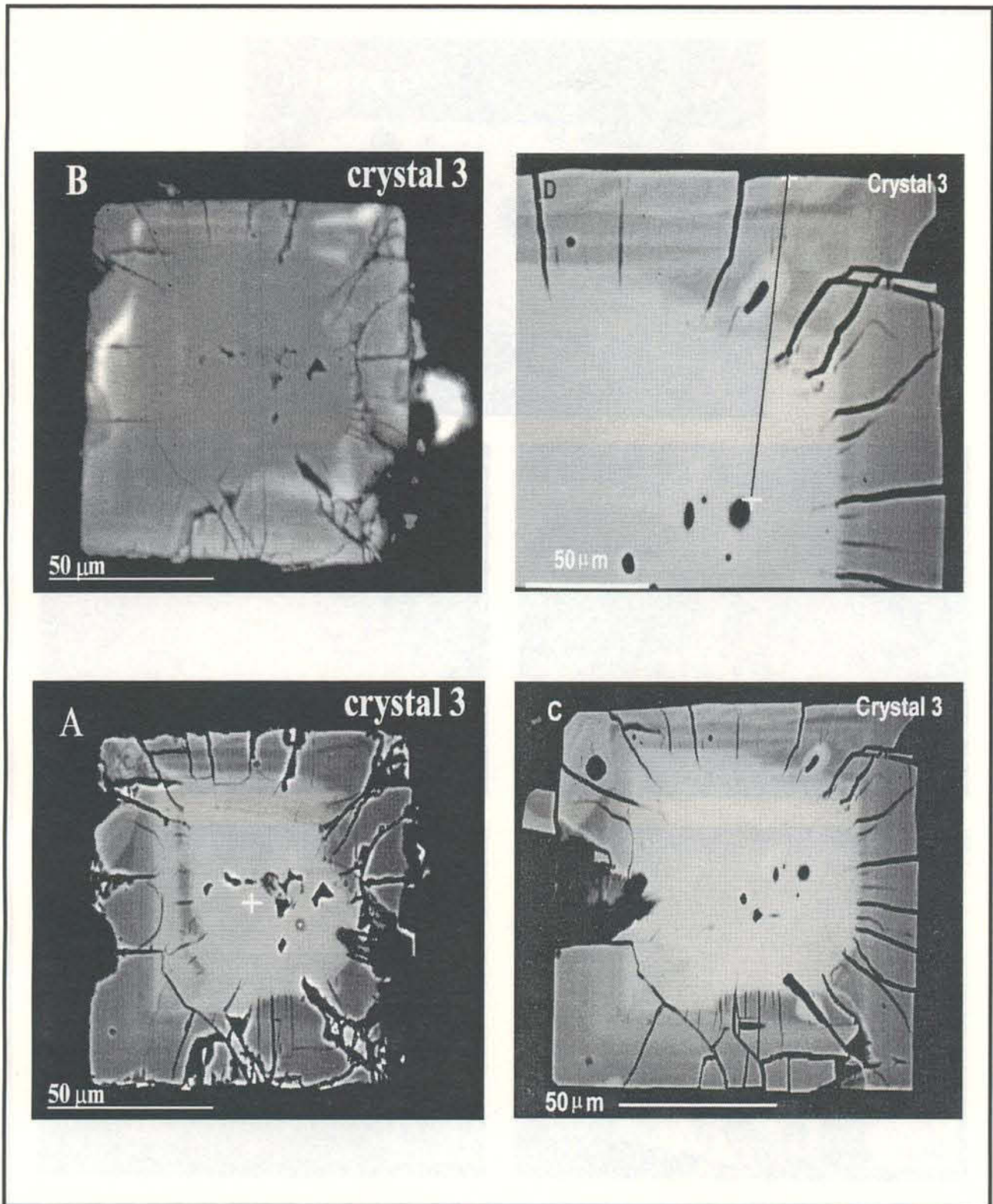


Figure 2 - Tuna Granite zircons cut perpendicular to *c* axis. 2A - BSE image shows large core taken by bright (in BSE) zircon, sealing fractures in places. 2B - CL image of the same section as 2A; fractures are less visible. 2C - BSE image: large core has different geometry than in Fig. 2A. 2D - Detail of 2C; inclusion is surrounded by bright (in BSE) zircon similar to the core; scan line indicated.

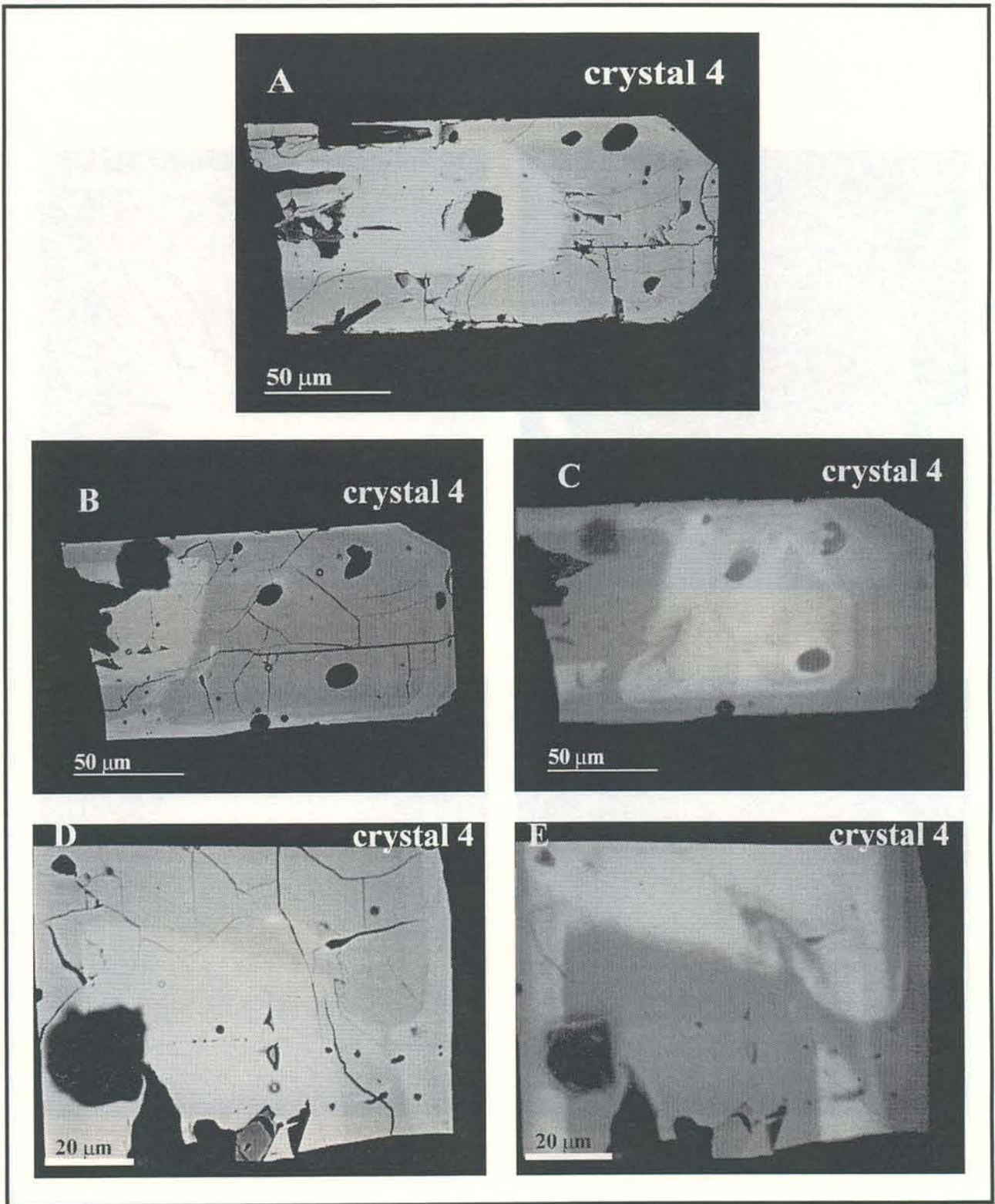


Figure 3 - São Sepé Granite zircon parallel to *c* axis. 3A - BSE image of euhedral (magmatic) crystal with a nearly euhedral core bright (in BSE). 3B - BSE image of repolished crystal 4; core does not have euhedral face parallel to *c* axis. 3C - CL image of same tomographic plane as 3B; bright regions in BSE becomes dark in CL signal; bright (in CL) portions circle some of the inclusions. 3D - Detail of 3B; a channel links bright (in BSE) core with bright (in BSE) rim; small worm-like bright portion seals fracture. 3E - CL image of same region as 3D; way distribution of bright (in CL) portion better explained by solid-state diffusion.

the pyramid or to the (001) face. It is observed on CL images that the diffusion process tends to homogenize portions of the crystal and expel the elements responsible for the luminescence (e.g. dark/CL in Figs. 1D, 2B and 3C).

Chemical traverses on three crystals are indicated in figures 1B, 1E and 2D, and the results shown in figure 4. There is very good correspondence between brightness of BSE image and chemical composition. The bright parts are all significantly enriched in U. In crystals 2 and 3, this enrichment is five-fold or more. One slightly brighter/BSE band on spot 3 of figure 1E is slightly enriched in U and very significantly in Y. In this crystal 2, Y does not follow U enrichment in the core as it does in crystal 3; in crystal 2, there is a high content of 1.37 wt% Y in the bright/BSE core. Such high Y contents have seldom been encountered in zircons, and seem to be typical of Pupin's (1992) "oceanic" granites (mantellic) such as the alkaline granites presently studied. Hf tends to be enriched by 20% in bright/BSE portions, as for instance in crystals 2 and 3.

INTERPRETATIONS AND CONCLUSIONS

Discordant fracture sealing was demonstrated by Hartmann *et al.* (1997) to occur as a young feature in an older crystal, and this is here found in all selected crystals from the two rock samples. Euhedral banding is usually considered as igneous zoning (Halden & Hawthorne, 1993; Hanchar & Miller, 1993; Vavra, 1994), particularly as observed in sections perpendicular to *c* axis (Benisek & Finger, 1993). In the present study, the concordant and discordant replacement are shown by chemical analyses to evolve into each other – sequential sections show the two features to merge in the images with the same chemical composition. They are therefore of metamorphic/metassomatic origin, not igneous. We demonstrate that euhedral banding is caused by enhancement of the previous crystal structure by introduction of elements (Hartmann & Vasconcellos, 1997). This explanation is an alternative to the proposal of Pidgeon (1992) that unzoned portions would be younger than zoned portions. We propose that the zircon crystals studied crystallized from a silicate liquid in a posttectonic environment. The rocks and contained crystals were affected by low-intensity, low grade, shear-zone deformation and metamorphism. The zircons were fractured during this external stress field, as observed on longitudinal and transversal fractures of crystals 1, 2 and 4. The fractures in crystal 3 are mostly radial and conform to the expansion model of Lee & Tromp (1995). Metamorphic shear-zone fluids percolated the crystals, exchanging many elements; Hf, Y, U contents are observed to be modified,

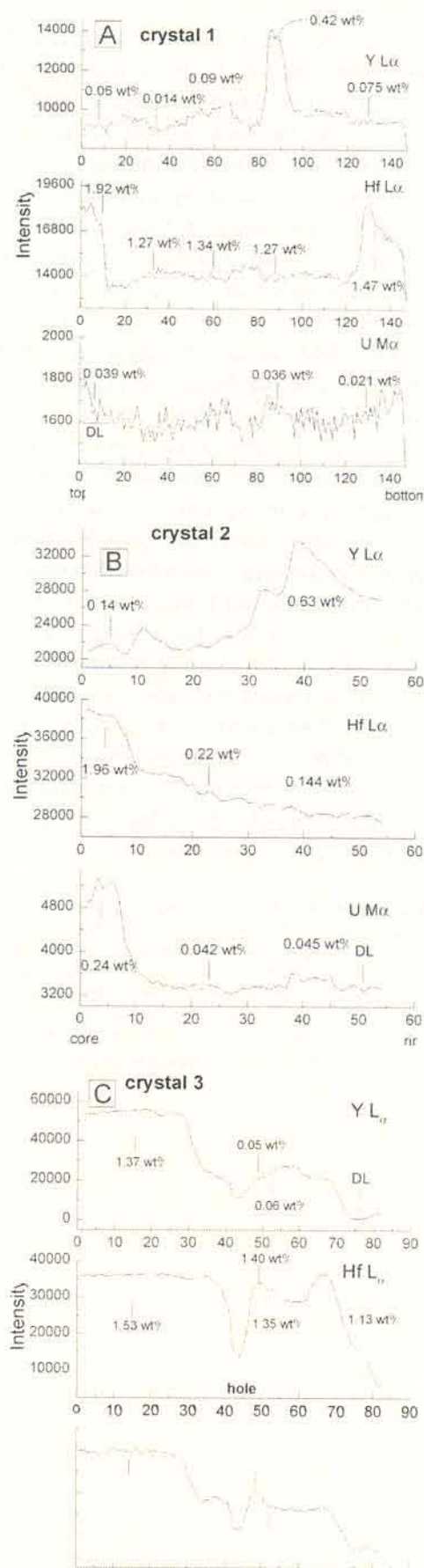


Figure 4 - Intensity vs distance diagrams for crystals 1, 2 and 3. Wt% WDS spot analyses indicated.

usually with increase of Hf, U and variable increase of Y in the metassomatized portions of the crystal. Short-circuit mechanisms allowed the cations to dislocate more rapidly and efficiently along the fractures, and we demonstrate that this transport evolved from the fractures into defect-rich euhedral bands. These bands were probably originally richer in U, Th and therefore more metamict. In portions of some crystals, a lattice-diffusion mechanism is present and even becomes dominant, transforming large volumes of old zircon into new zircon. The resulting textural aspect in BSE images is the presence of brighter discordant zones, euhedral bands and large volumes in cores or anywhere in the crystals.

The resulting chemical aspect is the increase in Hf, U in most younger bright parts and Y in some. This has far-reaching consequences in terms of the mineralogical, petrological and geochronological interpretation of zircon in igneous and metamorphic rocks – the chemistry of euhedral bands cannot be taken as representative of the liquid from which the crystal precipitated, the chemistry of the zircon may not be compared to the enclosing rock, and the ages obtained from isotopic determinations must be carefully evaluated. Zircon is a common igneous mineral, but its chemistry tends to be modified by metamorphic processes through introduction of several elements, including Hf, Y, U along fractures and defect-rich euhedral bands.

Acknowledgements – PADCT/FINEP/UFRGS supported the research, including the acquisition and installation of the electron microprobe laboratory at Centro de Estudos em Petrologia e Geoquímica, Instituto de Geociências, Universidade Federal do Rio Grande do Sul, in Porto Alegre, Brazil. Conselho Nacional do Desenvolvimento Científico e Tecnológico supported LAH and MAZV research and offered a scholarship to undergraduate geology student APR. Maria do Carmo Pinto Gastal is thanked for the zircon crystals, which she collected in the field and separated at UNESP. Paul Potter is thanked for the English review.

REFERENCES

- Babinski, M.; Chemale, F.; Hartmann, L.A.; Van Schmus, W.R. & Silva, L.C. da. 1996. Juvenile accretion at 750-700 Ma in Southern Brazil. *Geology*, **24** (5):439-442.
- Benisek, A. & Finger, F. 1993. Factors controlling the development of prism faces in granite zircons: a microprobe study. *Contributions to Mineralogy and Petrology*, **114**: 441-451.
- Gastal, M.C.P.; Schmitt, R.S. & Nardi, L.V.S. 1992. Granitóides da parte centro/sudoeste do Escudo Sul-riograndense. Novos dados e discussões sobre gênese e tipologia do magmatismo alcalino. *Pesquisas*, **19** (2):174-182.
- Halden, N.M. & Hawthorne, F.C. 1993. The fractal geometry of oscillatory zoning in crystals: Application to zircon. *American Mineralogist*, **78**: 1113-1116.
- Hanchar, J.M. & Miller, C.F., 1993. Zircon zonation patterns as revealed by cathodoluminescence and backscattered electron images: Implications for interpretation of complex crustal histories. *Chemical Geology*, **110**, 1-13.
- Hartmann, L.A.; Takehara, L.; Leite, J.D.; McNaughton, N. & Vasconcellos, M. 1997. Fracture sealing in zircon as evaluated by electron microprobe analyses and back-scattered electron imaging. *Chemical Geology*, **141**: 67-72.
- Hartmann, L. A. & Vasconcellos, M.A. Z. 1997. Metamorphic enhancement of the internal structure of zircon. In: EUG-9. *Terra Nova*, **9**:688.
- Lee, J.K.W. & Tromp, J., 1995. Self-induced fracture generation in zircon. *Journal of Geophysical Research*, **100** (B9):17,753-17,770.
- Leite, J.A.D.; Hartmann, L.A.; McNaughton, N.J. & Chemale Jr., F. 1998. SHRIMP U/Pb zircon geochronology of Neoproterozoic juvenile and crustal-reworked terranes in southernmost Brazil. *International Geology Reviews*, **40**: 688-705.
- Pidgeon, R.T. 1992. Recrystallization of oscillatory zoned zircon: some geochronological and petrological implications. *Contributions to Mineralogy and Petrology*, **110**: 463-472.
- Pupin, J.-P. 1992. Les zircons des granites océaniques et continentaux: couplage typologie-géochimie des éléments en traces. *Bulletin Société Géologique de France*, **163** (4): 495-507.
- Remus, M.V.D.; McNaughton, N.J.; Hartmann, L.A. & Fletcher, I.R. 1997. U-Pb SHRIMP zircon dating and Nd isotope data of granitoids of the São Gabriel Block, southern Brazil: evidence for an Archean/Paleoproterozoic basement. In: INTERNATIONAL SYMPOSIUM ON GRANITES AND ASSOCIATED MINERALIZATIONS, II., 1997, Salvador. *Anais...* Salvador, p. 271-272.
- Vavra, G., 1994. Systematics of internal zircon morphology in major Variscan granitoid types. *Contributions to Mineralogy and Petrology*, **117**: 331-344.